Inorganic Chemistry

ARTICLE

pubs.acs.org/IC

Blue-Light Emission of Cu(I) Complexes and Singlet Harvesting

Rafał Czerwieniec, Jiangbo Yu,[†] and Hartmut Yersin*

Institut für Physikalische und Theoretische Chemie, Universität Regensburg, Universitätstrasse 31, D-93040 Regensburg, Germany

Supporting Information

ABSTRACT: Strongly luminescent neutral copper(I) complexes of the type Cu(pop)(NN), with pop = bis(2-(diphenylphosphanyl)phenyl)ether and NN = bis(pyrazol-1-yl)borohydrate (pz_2BH_2), tetrakis(pyrazol-1-yl)borate (pz_4B), or bis(pyrazol-1-yl)-biphenyl-borate (pz_2Bph_2), are readily accessible in reactions of Cu(acetonitrile)$_4^+$ with equimolar amounts of the pop and NN ligands at ambient temperature. All products were characterized by means of single crystal X-ray diffractometry. The compounds exhibit very strong blue/white luminescence with emission quantum yields of up to 90%. Investigations of spectroscopic properties and the emission decay behavior in the temperature range between 1.6 K and ambient temperature allow us to assign the emitting electronic states. Below 100 K, the emission decay times are in the order of many hundreds of microseconds. Therefore, it is concluded that the emission stems from the lowest triplet state. This state is assigned to a metal-to-ligand charge-transfer state (^{3}MLCT) involving Cu-3d and pop-π^* orbitals. With temperature increase, the emission decay time is drastically reduced to e.g. to 13 s (Cu(pop)(pz_2Bph_2)) at ambient temperature. At this temperature, the complexes exhibit high emission quantum yields, as neat material or doped into poly(methyl methacrylate) (PMMA). This behavior is assigned to an efficient thermal population of a singlet state (being classified as ^{1}MLCT), which lies only 800 to 1300 cm^{-1} above the triplet state, depending on the individual complex. Thus, the resulting emission at ambient temperature largely represents a fluorescence. For applications in OLEDs and LEECs, for example, this type of thermally activated delayed fluorescence (TADF) creates a new mechanism that allows to harvest both singlet and triplet excitons (excitations) in the lowest singlet state. This effect of singlet harvesting leads to drastically higher radiative rates than obtainable for emissions from triplet states of Cu(I) complexes.

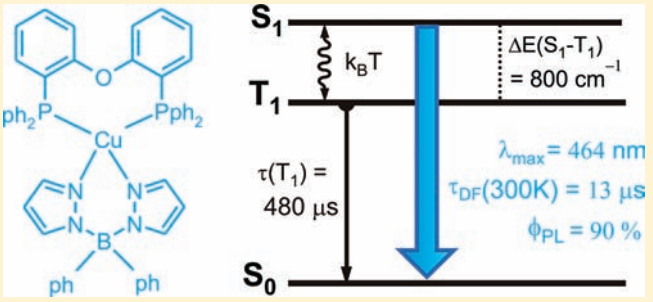

1. INTRODUCTION

During the past decades, properties of the lowest excited states of organo-transition metal complexes were extensively investigated. This was stimulated by the wide range of applications. In particular, luminescent materials are used as emitters in OLEDs (organic light emitting diodes),[1−6] in LEECs (light emitting electro-chemical cells),[7,8] as chemo- and biosensors,[9,10] and as lumophores for cell imaging.[11,12] Each of these applications imposes specific demands on the materials, such as chemical or electrochemical stability, color and color purity of the emitted light, high emission quantum yield, specific emission decay time, and so forth.

For example, complexes of heavy metal ions, such as cyclometalated iridium(III) complexes, are applied as particularly useful emitter materials for efficient light generation in electroluminescent devices. In such compounds, strong spin−orbit coupling (SOC) can weaken the spin-forbiddenness of the electronic transitions between the lowest excited triplet (T_1) and the singlet ground state (S_0).[13−15] Applying these materials, it is possible to harvest both the singlet and the triplet excitons ("triplet harvesting")[16−18] and to achieve an almost 100% internal electroluminescence efficiency.[19−21] This strategy is particularly successful for red and green light emitting OLEDs. However, the development of blue and white light emitting phosphorescent materials is still a challenge. The efficiency of blue phosphorescence from d^6 and d^8 transition metal complexes with suitably high lying excited triplet states depends strongly on the energy separation between the emitting state and higher lying metal centered dd* states. If the latter ones are thermally accessible at ambient temperature, that is, at an activation energy of 3000 to 3500 cm^{-1}, the luminescence is largely quenched.[22,23]

To overcome these difficulties, one can focus on complexes with a d^{10} ground state configuration, since low lying dd* states are not present. In this respect, Cu(I) complexes represent interesting materials. However, because of relatively weak spin−orbit coupling (SOC), emission decay times corresponding to the $T_1 \rightarrow S_0$ transitions are long, amounting to many hundreds of microseconds.[24−29] Compounds with such long emission decay times are not well suited for OLED applications since the roll-off of efficiency[30] would occur already at low current density. However, specific Cu(I) complexes exhibit a pronounced thermally activated delayed fluorescence at ambient temperature.[24,25,27,31] In these cases, the Boltzmann population of the lowest excited singlet state (S_1) manifests itself in a spectral blue shift and a prominent increase of the emission decay rate.

Received: April 20, 2011
Published: August 03, 2011

Table 1. Crystal Data, Data Collection, and Structure Refinement Details for Cu(pop)(pz_2BH_2), Cu(pop)(pz_4B), and Cu(pop)(pz_2Bph_2)

	1 Cu(pop)(pz_2BH_2) × CH_2Cl_2	**2** Cu(pop)(pz_4B) × $CH_3CO_2C_2H_5$	**3** Cu(pop)(pz_2Bph_2) × $CDCl_3$
crystal shape	plate	rod	prism
crystal color	colorless	colorless	colorless
empirical formula	$C_{42}H_{36}BCuN_4OP_2 \times CH_2Cl_2$	$C_{48}H_{40}BCuN_8O_3P_2 \times CH_3CO_2C_2H_5$	$C_{54}H_{44}BCuN_4OP_2, \times CDCl_3$
formula weight [g mol^{-1}]	833.97	881.18	1020.60
crystal size [mm]	0.180/0.110/0.050	0.6096/0.2610/0.0855	0.1616/0.1267/0.1129
crystal system	triclinic	triclinic	triclinic
space group	$P\bar{1}$	$P\bar{1}$	$P\bar{1}$
a [Å]	9.2753(3)	11.9642(3)	12.0809(6)
b [Å]	12.2741(5)	13.7264(4)	13.6212(6)
c [Å]	18.3819(4)	15.7278(5)	15.8676(7)
α [deg]	85.541(3)	105.349(3)	104.648(4)
β [deg]	89.870(2)	98.594(2)	97.265(4)
γ [deg]	71.762(3)	103.665(3)	101.654(4)
cell volume [$Å^3$]	1981.02(12)	2357.53(13)	2430.4(2)
Z	2	2	2
density [g cm^{-3}]	1.398	1.241	1.395
absorption coefficient [mm^{-1}]	3.093	1.637	3.124
F(000)	860	912	1052
T [K]	123	223	123
λ [Å]	1.54184	1.54184	1.54184
Θ range [deg]	2.41−62.14	3.49−76.63	3.46−73.19
reflections collected	20681	10995	17380
unique reflections	6163	9625	9428
observed reflections [$I > 2\sigma(I)$]	4753	8672	7729
absorption correction	multiscan	analytical	analytical
GOF	0.986	1.081	1.051
final R_1 [$I \geq 2\sigma(I)$]	0.0513	0.0365	0.0387
wR_2	0.1302	0.1031	0.0968

This leads frequently also to an increase of the emission quantum yield as compared to the triplet emission. Therefore, in spite of the pronounced spin-forbiddenness of the $T_1 \rightarrow S_0$ transition, such Cu(I) complexes represent attractive candidates to be applied in electroluminescent devices. In particular, the mechanism of the thermally activated fluorescence allows to harvest both singlet and triplet excitons and leads to the singlet harvesting effect.[32−34] In this contribution, we present syntheses and crystal structures and discuss photophysical properties of a new class of copper(I) complexes. Their application as blue/white emitter materials in OLEDs is proposed.

2. EXPERIMENTAL SECTION

2.1. Syntheses. Tetrakis(acetonitrile)copper(I) hexafluorophosphate, bis(2-(diphenylphosphanyl)phenyl) ether (pop), potassium dihydrobis(pyrazol-1-yl)borate (Kpz_2BH_2), potassium tetrakis(pyrazol-1-yl)borate (Kpz_4B), and potassium diphenyl-bis(pyrazol-1-yl)borate (Kpz_2Bph_2) were purchased from Sigma-Aldrich and were used as obtained. The complexes Cu(pop)(pz_2BH_2) (**1**), Cu(pop)(pz_4B) (**2**), and Cu(pop)(pz_2Bph_2) (**3**) were prepared according to the following general procedure. Equimolar amounts (0.1 mmol) of tetrakis(acetonitrile)copper(I) hexafluorophosphate and (2-(diphenylphosphanyl)-phenyl)ether were dissolved in 50 mL of acetonitrile, and the solution was stirred under nitrogen at room temperature. After 2 h a potassium salt of respective bis-pyrazolyl ligand (0.1 mmol) was added, and the reaction mixture was stirred for another 2 h to form a colorless precipitate. The solid was filtered off, washed with water, acetonitrile, and diethyl ether. Then it was dissolved in a small amount of dichloromethane and passed through a short column with neutral aluminum oxide. The solvent was removed, and the product dried in vacuum. Single crystals of Cu(pop)-(pz_2BH_2) (**1**), Cu(pop)(pz_4B) (**2**), and Cu(pop)(pz_2Bph_2) (**3**) for X-ray diffraction measurements were obtained from dichloromethane/hexane, ethyl acetate, and chloroform-D_1, respectively.

Cu(pop)(pz_2BH_2) (***1***). Yield 84%. ^{1}H NMR (300 MHz, CD_2Cl_2): *δ* 7.57 (d, 2H), 7.09−7.28 (m, 22H), 6.81−6.92 (m, 6H), 6.65−6.71 (m, 2H), 5.87 (t, 2H), 3.30−4.20 (br, 2H). $^{13}C\{^1H\}$NMR (75 MHz, CD_2Cl_2): *δ* 103.1, 120.7, 124.7, 125.8, 127.0, 128.35, 128.4, 128.47, 129.4, 131.2, 132.9, 134.2, 134.3, 134.35, 134.39, 136.8, 141.4. $^{31}P\{^1H\}$ (121 MHz, CD_2Cl_2): *δ* −18.7 (s). MS (ES): *m*/*z* 749.3 (MH^+). Found: C, 61.72; H, 4.52; N, 6.72%. $C_{43}H_{36}BCuN_4OP_2Cl_2$ requires: C, 62.08; H, 4.36; N, 6.73%.

Cu(pop)(pz_4B) (***2***). Yield 84%.^{1}H NMR (300 MHz, CD_2Cl_2): *δ* 7.38 (s, 4H), 7.22−7.29 (m, 4H), 7.10−7.19 (m, 10), 6.78−6.98 (m, 16H), 6.68−6.75 (m, 2H), 5.89 (t, 4H). $^{13}C\{^1H\}$NMR (75 MHz, CD_2Cl_2): *δ* 104.4, 120.8, 124.8, 128.57, 128.64, 128.68, 128.6, 131.4, 133.2, 132.4, 132.6, 134.25, 134.37, 134.54, 135.6, 141.9, 158.4. $^{31}P\{^1H\}$ (121 MHz, CD_2Cl_2): *δ* −15.0 (s). MS (ES): *m*/*z* 881.4 (MH^+). Found: C, 65.11; H, 4.82; N, 12.83%. $C_{48}H_{40}BCuN_8OP_2$ requires: C, 65.42; H, 4.57; N, 12.72%.

Cu(pop)(pz_2Bph_2) (***3***). Yield 84%.^{1}H NMR (300 MHz, CD_2Cl_2): *δ* 7.21−7.28 (m, 4H), 7.04−7.19 (m, 14H), 6.83−6.97 (m, 20H), 6.73−6.79 (m, 4H), 5.84 (t, 2H). $^{13}C\{^1H\}$NMR (75 MHz, CD_2Cl_2):

dx.doi.org/10.1021/ic200811a |*Inorg. Chem.* 2011, 50, 8293–8301

δ 103.1, 120.7, 124.7, 125.8, 127.0, 127.2, 128.4, 129.4, 131.2, 132.7, 132.9, 133.1, 134.2, 134.3, 134.35, 134.4, 136.9, 141.4. $^{31}P\{^{1}H\}$ (121 MHz, CD_2Cl_2): δ −15.4 (s). MS (ES): *m/z* 881.4 (MH^+). Found: C, 71.53; H, 5.10; N, 6.62%. $C_{54}H_{44}BCuN_4OP_2$ requires: C, 71.96; H, 4.92; N, 6.22%.

2.2. Crystal Structures. Diffraction data were collected with an Oxford Diffraction Gemini Ultra CCD diffractometer with Cu−K_α radiation (λ = 1.54184 Å). The structures were resolved by direct methods (SIR-97)[35] and refined by full-matrix least-squares on F^2 using the SHELXL-97 program.[36] The H atoms were calculated geometrically, and a riding model was applied during the refinement process. In the crystal of Cu(pop)(pz_4B) a disordered solvent molecule was found which could not be well refined. However, the effect of this disorder did not have any significant impact on conclusions concerning the structure of the Cu(pop)(pz_4B) molecule. In this case, the volume (299.1 $Å^3$) and the approximate electron number (44) of the solvent molecule were determined using the SQEEZE program.[37] The crystallographic and refinement data are collected in Table 1.

2.3. Instrumentation and Spectroscopic Methods. Elemental analyses were performed with a Vario EL III element analyzer. NMR and ES-MS spectra were recorded using a Bruker Avance III 300 MHz and a Finnigan MAT SSQ 710 A spectrometer, respectively.

UV−vis absorption spectra were recorded for dilute dichloromethane solutions ($c \approx 5 \times 10^{-5}$ M) using a Varian Cary 300 double beam spectrometer. Luminescence properties of Cu(pop)(pz_2BH_2) (**1**), Cu(pop)(pz_4B) (**2**), and Cu(pop)(pz_2Bph_2) (**3**) in degassed dichloromethane solution ($c \approx 10^{-5}$ M) and in spin-coated poly(methyl methacrylate) (PMMA) films (≈1 weight % of the complex) were investigated at ambient temperature. Powder samples were studied in the temperature range between 1.6 and 300 K. Ambient temperature luminescence spectra were recorded with a Horiba Jobin Yvon Fluorolog 3 steady-state fluorescence spectrometer. This spectrometer was modified to allow for measurements of emission decay times. As excitation source a nitrogen laser (λ_{exc} = 337.1 nm, pulse duration = 4 ns) was used. The emission was detected with a photomultiplier attached to a FAST ComTec multichannel scaler PCI card with a time resolution of 250 ps. Photoluminescence (PL) quantum yields were determined using a Hamamatsu system for absolute PL quantum yield measurements (type C9920−02) equipped with an integrating sphere with Spectralon inner surface coating. The samples were carefully degassed by at least five freeze-pump-thaw cycles (compare ref 13). Experiments at low temperatures were performed in a helium cryostat (Cryovac Konti Cryostat IT) in which the helium gas flow, gas pressure, and heating were controlled. In this equipment, spectra were registered with a Hamamatsu C9920 multi channel detector, and emission decay curves were recorded with a cooled photomultiplier (RCA C7164R) attached to a TR 555 tripple monochromator (Spectroscopy & Imaging GmbH) and a FAST ComTec PCI card. As excitation source, a pulsed Nd:YAG laser (IB Laser Inc., DiNY pQ 02) with an excitation wavelength of λ_{exc} = 355 nm (third harmonic) or a pulse width of about 7 ns was applied.

3. RESULTS AND DISCUSSION

3.1. Syntheses and Crystal Structures. Cu(pop)(pz_2BH_2) (**1**), Cu(pop)(pz_4B) (**2**), and Cu(pop)(pz_2Bph_2) (**3**) were prepared in a conventional way by reacting $Cu(CH_3CN)_4^+$ with equimolar amounts of the bisphosphine and bispyrazolyl ligands. In the course of these reactions, the weakly coordinating acetonitrile ligands were replaced by the chelating ligands according to the reaction scheme shown in Figure 1. The obtained compounds are stable in air at least for several months.

Cu(pop)(pz_2BH_2) (**1**), Cu(pop)(pz_4B) (**2**), and Cu(pop)(pz_2Bph_2) (**3**) crystallize in the triclinic $P\bar{1}$ space group with

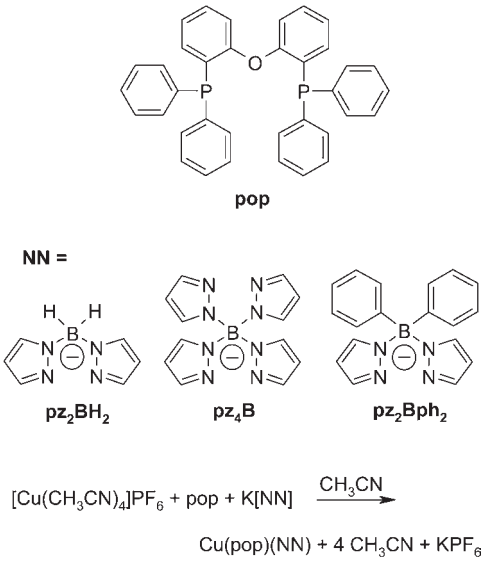

Figure 1. Reaction scheme and ligands used.

the molecules of the complex packed as centrosymmetric head-to-tail dimers. The crystals contain also molecules of the solvent used for crystallization. ORTEP plots of the Cu(pop)(pz_2BH_2), Cu(pop)(pz_4B), and Cu(pop)(pz_2Bph_2) molecules are shown in Figure 2, and the major structural parameters are listed in Table 2. The X-ray crystallographic studies reveal that the metal ions in these complexes exhibit highly distorted tetragonal coordination. In particular, the small N−Cu−N angles of 95.51(6)−96.45(8)° and P−Cu−N angles ranging from 103.20(10) to 126.94(6)° deviate strongly from the tetrahedral value of 109.5°. This situation reflects the specific steric requirements of the pop and NN ligands. Interestingly, the molecular geometries are stabilized by intramolecular ππ-stacking interactions, involving one phenoxy ring and one of the phenyl rings of the pop ligand. A similar situation is found in many other transition metal complexes with the pop ligand.[38−40]

3.2. Photophysical Properties at Ambient Temperature. Figure 3 shows UV−vis absorption spectra of the complexes Cu(pop)(pz_2BH_2) (**1**), Cu(pop)(pz_4B) (**2**), and Cu(pop)(pz_2Bph_2) (**3**) together with the spectra of the free ligands pop and $pz_2BH_2^-$. The copper(I) complexes display intense absorption bands with maxima between 265 and 275 nm. These are assigned to spin allowed π−π* transitions of the pop ligand, while the ligand centered transitions of $pz_2BH_2^-$ are expected to occur at shorter wavelengths (see Figure 3). At longer wavelengths, the complexes display additional bands (ε(320 nm) = 7000 to 9200 M^{-1} cm^{-1}) between about 310 and 370 nm. Since analogous absorptions are not present either in pop or in the bis(pyrazol-1-yl)borate ligands, these low energy absorptions are assigned to spin allowed d-π* transitions involving mainly the 3d orbitals of Cu(I) and the π* orbitals of the pop ligand. This conclusion is also supported by results of density functional theory (DFT) calculations on Cu(pop)(pz_2BH_2) predicting the highest occupied and the lowest unoccupied orbitals of the complex being largely of metal 3d and pop π* character, respectively.[41] The assignment of the emission of the discussed Cu(pop)(NN) complexes as stemming from such a metal-to-ligand charge-transfer (MLCT) excited state (involving the pop π* orbitals) is also consistent with the influence of ligand modifications on the emission properties. In particular, replacement of

dx.doi.org/10.1021/ic200811a |*Inorg. Chem.* 2011, 50, 8293–8301

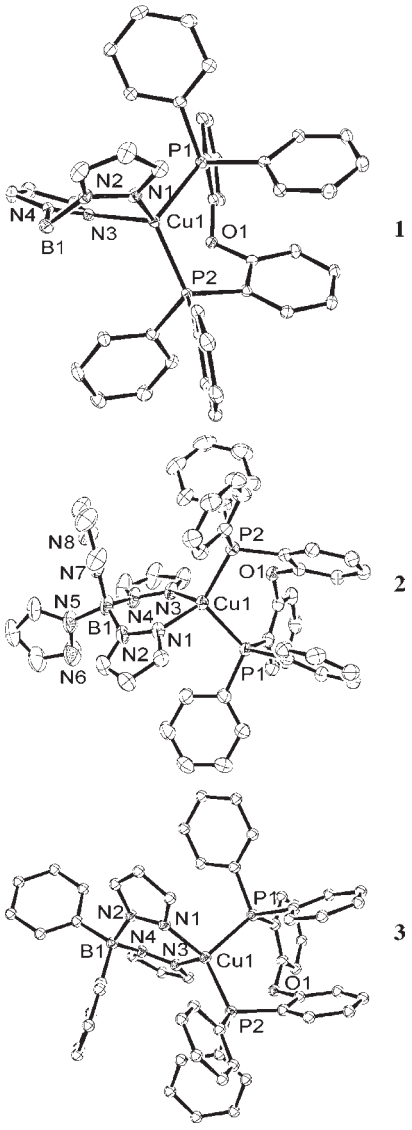

Figure 2. Crystallographic view (thermal ellipsoid with 30% probability) of **1** Cu(pop)(pz_2BH_2), **2** Cu(pop)(pz_4B), and **3** Cu(pop)-(pz_2Bph_2) and atom numbering schemes. Hydrogen atoms and solvent molecules are omitted for clarity.

the pop ligand by another bisphosphine ligand results in a significant change of the absorption and luminescence properties of the resulting complex. For instance, neat Cu(dppb)(pz_2BH_2) (with dppb = 1,2-bis(diphenylphosphino)benzene) exhibits at ambient temperature an emission with λ_{max} = 570 nm,[41] as compared to the λ_{max} values of Cu(pop)(pz_2BH_2) (**1**), Cu-(pop)(pz_4B) (**2**), and Cu(pop)(pz_2Bph_2) (**3**) lying between 436 and 464 nm (see below, Table 3). On the other hand, substitutions on the bis(pyrazol-1-yl)borate ligands lead only to minor spectral shifts. Even replacement of the bis(pyrazol-1-yl)borate ligand by acac = acetylacetonate results only in a small change of the emission color. For example, for neat Cu(pop)(acac), a λ_{max} value of 461 nm was reported.[42]

The emission spectra of Cu(pop)(pz_2BH_2), Cu(pop)(pz_4B), and Cu(pop)(pz_2Bph_2) are broad and unstructured, which is in accordance with the MLCT nature of the emitting state. Moreover, the luminescence properties strongly depend on the environment. For instance, as depicted in Figure 4,

Table 2. Selected Structural Parameters for the Complexes Cu(pop)(pz_2BH_2), Cu(pop)(pz_4B), and Cu(pop)(pz_2Bph_2)

	1 Cu(pop)-(pz_2BH_2)	**2** Cu(pop)-(pz_4B)	**3** Cu(pop)-(pz_2Bph_2)
	Distances [Å]		
Cu1−P1	2.2704(4)	2.2925(4)	2.2957(6)
Cu1−P2	2.2348(4)	2.2319(5)	2.2203(6)
Cu1−N1	2.0501(12)	2.0444(17)	2.0290(20)
Cu1−N3	2.0355(13)	2.0251(14)	2.0197(18)
	Bond Angles [deg]		
P1−Cu1−P2	112.15(2)	110.26(2)	109.20(2)
N1−Cu1−N3	96.14(5)	95.51(6)	96.45(8)
P1−Cu1−N1	103.29(4)	106.06(5)	103.20(10)
P1−Cu1−N3	108.37(4)	107.79(5)	107.07(6)
P2−Cu1−N1	121.63(4)	125.25(5)	126.94(6)
P2−Cu1−N3	113.54(4)	110.20(5)	112.11(6)

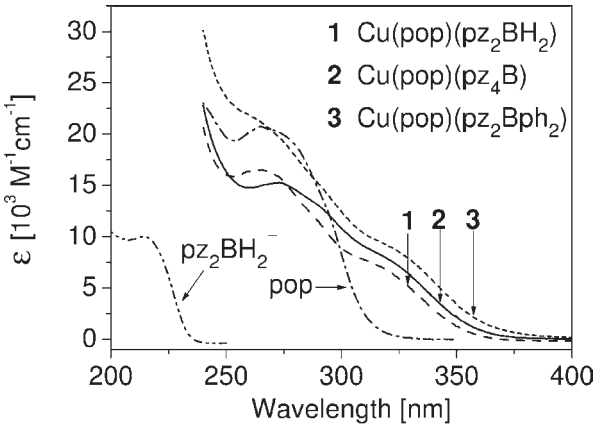

Figure 3. Absorption spectra of the Cu(I) complexes and free ligands measured at ambient temperature. Spectra of **1** Cu(pop)(pz_2BH_2), **2** Cu(pop)(pz_4B), **3** Cu(pop)(pz_2Bph_2), and pop were recorded in dichloromethane. Kpz_2BH_2 was measured in an acetonitrile solution.

Cu(pop)(pz_2BH_2) shows a blue emission (λ_{max} = 436 nm) as neat material, a white-blue emission (λ_{max} = 462 nm) in PMMA, and a green emission (λ_{max} = 535 nm) in dichloromethane solution. This red shift is accompanied by a considerable reduction of the emission quantum yield and a shortening of the emission decay time. Similar trends are also observed for the other two complexes Cu(pop)(pz_4B) (**2**) and Cu(pop)-(pz_2Bph_2) (**3**) (Table 3). These observations can be explained by changes of the molecular geometry of the Cu(I) compounds which take place after MLCT excitation. In the electronic ground state (d^{10} configuration), the complexes display a pseudotetragonal coordination of the metal ion, whereas in the MLCT excited state, with a d^9 configuration of the metal ion, a flattening distortion of the molecular structure occurs.[26,27,43−46] In crystalline environments (neat samples) of Cu(pop)(pz_2BH_2) (**1**), Cu(pop)(pz_4B) (**2**), and Cu(pop)(pz_2Bph_2) (**3**), λ_{max} values of 436, 447, and 464 nm and ϕ_{PL} values of 45, 90, and 90%, respectively, are found. In a moderately rigid environment of a PMMA film, the emission maxima are found at λ_{max} = 462, 457, and 466 nm, respectively. The emission quantum yields drop, but they are still higher than 30%. In fluid dichloromethane solution,

dx.doi.org/10.1021/ic200811a |*Inorg. Chem.* 2011, 50, 8293–8301

Table 3. Luminescence Properties of Cu(pop)(pz_2BH_2), Cu(pop)(pz_4B), and Cu(pop)(pz_2Bph_2) in Different Matrixes at Ambient Temperature

1 Cu(pop)(pz_2BH_2) **2** Cu(pop)(pz_4B) **3** Cu(pop)(pz_2Bph_2)

Emission properties:	λ_{max} [a] [nm]	τ [b] [μs]	ϕ_{PL} [c] [%]	CIE 1931 [d] {x;y}	λ_{max} [a] [nm]	τ [b] [μs]	ϕ_{PL} [c] [%]	CIE 1931 [d] {x;y}	λ_{max} [a] [nm]	τ [b] [μs]	ϕ_{PL} [c] [%]	CIE 1931 [d] {x;y}
powder:	436	20	45	{0.15; 0.11}	447	22	90	{0.14; 0.11}	464	13	90	{0.16; 0.22}
PMMA:	462	22	35	{0.17; 0.21}	457	24	30	{0.17; 0.18}	466	23	41	{0.17; 0.21}
CH_2Cl_2:	535	1.3	9	{0.35; 0.47}	500	0.5	2	{0.26; 0.38}	498	1.8	8	{0.25; 0.39}

[a] λ_{max} = emission maximum (error ±2 nm). [b] τ = emission decay time (monoexponential fit) measured after pulsed excitation at 337.1 nm (relative error ±5%). [c] ϕ_{PL} = photoluminescence quantum yield (relative error ±5%). [d] CIE 1931 color space coordinates (see ref 54).

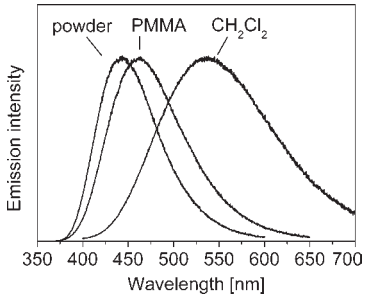

Figure 4. Luminescence spectra of Cu(pop)(pz_2BH_2) (**1**) as powder, in a PMMA film ($c \approx 1$ weight %), and in degassed dichloromethane ($c \approx 5 \times 10^{-5}$ mol/L). Spectra were taken at ambient temperature.

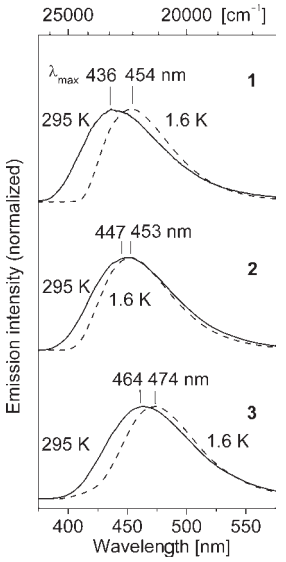

Figure 5. Luminescence spectra of Cu(pop)(pz_2BH_2) (**1**), Cu(pop)-(pz_4B) (**2**), and Cu(pop)(pz_2Bph_2) (**3**) powders at different temperatures (λ_{exc} = 355 nm). Emission maxima are marked for T = 1.6 (dashed lines) and 295 K (solid lines). The energy scale [cm^{-1}] is shown for orientation.

where large rearrangements of the molecular geometry can take place, the emission maxima are distinctly red-shifted to λ_{max} = 535 nm (**1**), 500 nm (**2**), and 498 nm (**3**) with ϕ_{PL} values below 10%. A pronounced distortion of the molecular geometry results in an increase of radiationless deactivation according to a better overlap of ground state and excited state vibrational wave functions.[47,48] Additionally, the resulting smaller energy gap induces a further increase of the radiationless decay rate (energy gap law).[49,50] Obviously, in a rigid environment, such distortions are largely suppressed. Thus, for the studied complexes, high emission quantum yields are observed in the solid state and in a rigid polymer matrix. A similar behavior has already been reported for several cationic copper(I) complexes.[51−53]

Interestingly, steric demands of the ligands can also reduce the extent of excited state distortions. This can be seen for the studied series of compounds. The largest red shift of the emission, caused by a change of the environment from powder (crystalline environment) to solution, is found for Cu(pop)(pz_2BH_2) (**1**) with the relatively small ligand $pz_2BH_2^-$, while for complexes with bulkier ligands, pz_4B^- and $pz_2Bph_2^-$, the shifts of the emission maxima are significantly smaller (Table 3). However, the steric hindrances induced by the phenyl and pyrazolyl groups in pz_4B^- and $pz_2Bph_2^-$ are not sufficient to completely prevent distortions of the molecular structures of Cu(pop)(pz_4B) (**2**) and Cu(pop)-(pz_2Bph_2) (**3**) after excitation.

For completeness, it is remarked that the very high ϕ_{PL} values obtained for the studied complexes in the solid state indicate that effects of energy transfer between adjacent emitter molecules as well as triplet−triplet annihilation do not seem to be important. This can be rationalized by assuming at least a small geometry change in the excited state even for the neat material. Accordingly, the resonance condition required for the occurrence of energy transfer processes between excited and nonexcited

dx.doi.org/10.1021/ic200811a |Inorg. Chem. 2011, 50, 8293–8301

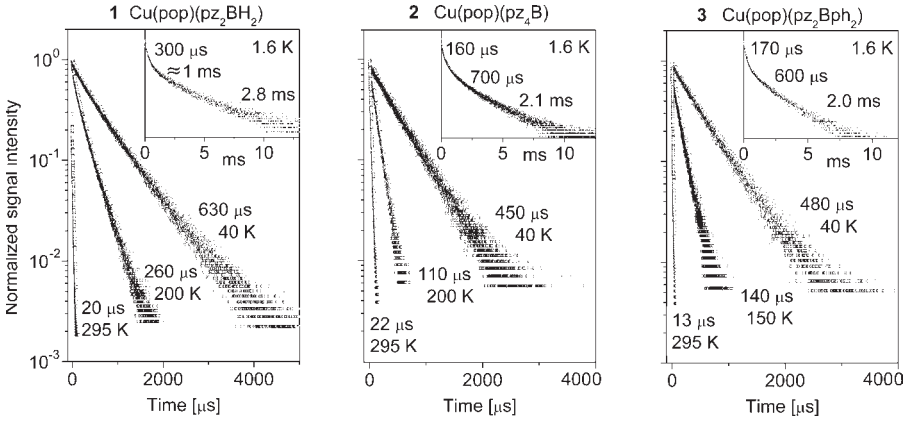

Figure 6. Emission decay of neat Cu(pop)(pz_2BH_2) (**1**), Cu(pop)(pz_4B) (**2**), and Cu(pop)(pz_2Bph_2) (**3**) at different temperatures measured after pulsed excitation at λ_{exc} = 355 nm and detected at 450 nm (Cu(pop)(pz_2BH_2) and Cu(pop)(pz_4B)) and at 470 nm (Cu(pop)(pz_2Bph_2)), respectively.

complexes is no longer fulfilled. Consequently, emission self-quenching and quenching by triplet−triplet annihilation become less probable.

3.3. Triplet State Emission. Figure 5 shows luminescence spectra of Cu(pop)(pz_2BH_2) (**1**), Cu(pop)(pz_4B) (**2**), and Cu(pop)(pz_2BH_2) (**3**) measured as powders at 1.6 K. The spectra are broad and unstructured. With temperature increase to about 150 K, the emission maxima do not shift significantly. They lie at 454 nm (**1**), 453 nm (**2**), and 474 nm (**3**), respectively. With further temperature increase, the spectra gradually become broader and a blue shift of the emission bands is observed. These effects are explained in Section 3.4.

Figure 6 displays the emission decay behavior at different temperatures. At T = 1.6 K, the decay curves are distinctly nonexponential. For example, for Cu(pop)(pz_2Bph_2) (**3**), the decay can be described by a triexponential decay function with individual components of 170 μs, 600 μs, and 2 ms. Comparable decay times are also found for Cu(pop)(pz_4B) (**2**) with 160 μs, 700 μs, and 2.1 ms, and for Cu(pop)(pz_2BH_2) (**1**)[55] with 300 μs, ≈1 ms, and 2.8 ms. These three different components are most likely related to the three substates of the lowest triplet state T_1. The splitting of the T_1 state, that is, the zero-field splitting (ZFS), could not be determined, since the spectra are too broad. However, the amount of the corresponding splitting, representing the energy separation between the lowest and the highest T_1 substate, is expected to be significantly smaller than typically found for Ir(III) or Pt(II) organometallic complexes.[13−15,56−59] For Cu(I) complexes, with the spin−orbit coupling (SOC) constant of copper being about five times smaller than that of iridium or platinum,[60] ΔE(ZFS) values of the order of 1 to 10 cm^{-1} are expected (compare ref 28). For such small energy separations between the triplet sublevels, the spin−lattice relaxation (SLR) processes between the T_1 substates are relatively slow at T = 1.6 K.[57] In particular, if the SLR times are much longer than the decay times of the transitions to the ground state, each substate emits according to its individual decay time. Such a situation is frequently found for ΔE(ZFS) values of less than 1 or 2 cm^{-1}.[57,58,61] Thus, we identify the decay components, determined at T = 1.6 K (see the insets of Figure 6), to represent approximately the individual decay times of different triplet substates.

With temperature increase, the SLR processes become faster. This leads to a thermal equilibration of the T_1 substate

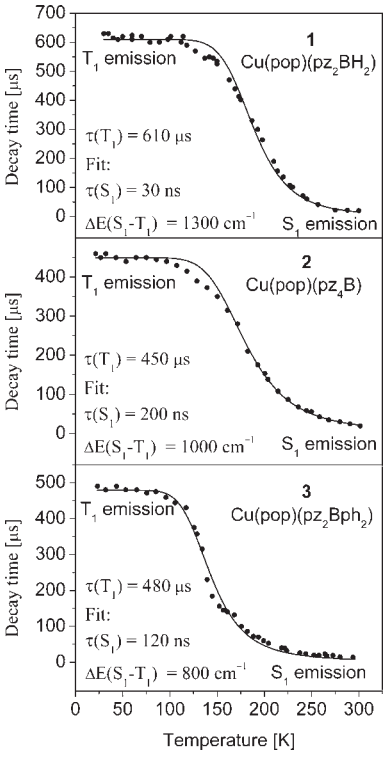

Figure 7. Emission decay time of Cu(pop)(pz_2BH_2), Cu(pop)(pz_4B), and Cu(pop)(pz_2Bph_2) powders. The complexes were excited with a pulsed UV laser (pulse width 7 ns) at λ_{exc} = 355 nm. The emission was detected at λ_{det} = 450 nm (Cu(pop)(pz_2BH_2) and Cu(pop)(pz_4B)) and at 470 nm (Cu(pop)(pz_2Bph_2)), respectively. The solid lines represent fits of eq 1 to the experimental data.

populations. As a consequence, the compound emit according to an averaged decay time. This situation is found for the studied complexes at temperatures above 30 K. Between 30 K and about 100 K, the measured decay times are almost constant and a plateau is found at values of 610 (**1**), 450 (**2**), and 480 μs (**3**), respectively (Figure 7).

3.4. Thermal Activation of the Lowest Singlet State. As discussed above, below T = 100 K, the luminescence originates from the lowest triplet state. However, for T > 100 K, the decay time becomes distinctly shorter (Figure 7). This behavior,

dx.doi.org/10.1021/ic200811a |*Inorg. Chem.* 2011, 50, 8293–8301

Table 4. Energies and Decay Times for the Investigated Cu(I) Complexes

	Cu(pop) (pz_2BH_2) (**1**)	Cu(pop) (pz_4B) (**2**)	Cu(pop) (pz_2Bph_2) (**3**)
$E(T_1)^a$	23800 cm^{-1}	24000 cm^{-1}	23200 cm^{-1}
$E(S_1)^b$	25100 cm^{-1}	24700 cm^{-1}	24000 cm^{-1}
$\Delta E(S_1-T_1)^c$	1300 cm^{-1}	1000 cm^{-1}	800 cm^{-1}
$\tau_I{}^d$	2.8 ms	2.1 ms	2.0 ms
$\tau_{II}{}^d$	≈ 1 ms	700 μs	600 μs
$\tau_{III}{}^d$	300 μs	160 μs	170 μs
$\tau(T_1)^e$	610 μs	450 μs	480 μs
$\tau(S_1)^f$	30 ns	200 ns	120 ns

[a] $E(T_1)$: energy determined from the high energy flank of the phosphorescence spectra (at 15% of the peak intensity) at 40 K. [b] $E(S_1)$: energy determined from the high energy flank of the fluorescence spectra (at 15% of the peak intensity) at ambient temperature. [c] $\Delta E(S_1-T_1)$: activation energy as determined from a fit of eq 1) to the measured decay times (see Figure 7). [d] τ_I, τ_{II}, and τ_{III} are the decay components of the T_1 substates determined from the emission decay at $T = 1.6$ K (see Figure 6). [e] $\tau(T_1)$: decay time of the T_1 state at 30 K < T < 100 K (plateau). [f] $\tau(S_1)$: decay time of the S_1 state determined from a fit of eq 1 to the measured decay times (see Figure 7).

together with the blue shift of the luminescence spectra (Figure 5), indicates that a higher lying electronic state with a distinctly larger deactivation rate becomes involved. In analogy to several other Cu(I) complexes,[24−28,31] this higher lying state is assigned as the lowest excited singlet state S_1, being of ^{1}MLCT character. Above $T \approx 250$ K, this singlet emission strongly dominates. It represents a thermally activated delayed fluorescence. Under the assumption of a fast thermalization between the T_1 and the S_1 state the decay time of this two-state system can be approximated to (compare analogous treatments in refs 13 and 59) for a three-state model system

$$\tau_{av} = \frac{1 + \exp(-\Delta E(S_1-T_1)/k_B T)}{1/\tau(T_1) + 1/\tau(S_1)\exp(-\Delta E(S_1-T_1)/k_B T)} \quad (1)$$

Herein k_B is the Boltzmann constant, $\tau(T_1)$ and $\tau(S_1)$ are the intrinsic decay times of the emitting triplet and singlet state, respectively, and $\Delta E(S_1-T_1)$ is the energy separation (activation energy) between these two states. For the studied Cu(I) complexes, the $\tau(T_1)$ lifetimes correspond to the values of the plateaus at temperatures between 30 and about 100 K. By fitting eq 1 to the measured decay times, the $\tau(S_1)$ and $\Delta E(S_1-T_1)$ values are obtained. The respective fit parameters are depicted in Figure 7 and summarized in Table 4.

Results of the analysis give insight into the properties of the emitting excited states. In particular, the $\Delta E(S_1-T_1)$ values found for the investigated copper(I) complexes lie between 800 and 1300 cm^{-1}. These values fit well to the energy separations as determined from the emission spectra (Figure 5 and Table 4). The corresponding energy separations are small as compared to many other compounds. For example, the lowest singlet and triplet $\pi\pi^*$ states of the free pop ligand are separated by more than 6000 cm^{-1},[62] while for Pt(2-thpy)$_2$ (with 2-thpy = 2-thienylpyridinate) a $\Delta E(S_1-T_1)$ value of ≈3300 cm^{-1} was determined.[58] The emitting triplet state of this latter compound was assigned to be a ligand centered state of $\pi\pi^*$ character with significant MLCT contributions. Thus, the small $\Delta E(S_1-T_1)$ values found for the Cu(I) complexes can be rationalized by a distinct charge transfer from the metal center to the ligand. In such a situation of a pronounced charge separation upon excitation, the exchange interaction becomes small and consequently also the singlet−triplet splitting. This is a well-known effect, which explains also the small splitting between the $^1n\pi^*$ and $^3n\pi^*$ states of organic molecules[47] (compare also ref 58). For completeness, it is mentioned that the emission decay times determined for the singlet state S_1, lying between 30 and 200 ns (Table 4), are longer than found for decay times of allowed $S_1 \rightarrow S_0$ transitions of organic molecules.[47] Obviously, for the studied Cu(I) compounds, the corresponding transition probabilities are relatively low.

4. SINGLET HARVESTING AND CONCLUDING REMARKS

The analysis of the emission behavior of Cu(pop)(pz_2BH_2) (**1**), Cu(pop)(pz_4B) (**2**), and Cu(pop)(pz_2Bph_2) (**3**) shows that the luminescence of these compounds at ambient temperature represents a delayed fluorescence stemming from the thermally populated singlet state S_1. In other words: the emission at T = 300 K is nearly completely a $S_1 \rightarrow S_0$ fluorescence, but the S_1 state is thermally populated by the reservoir of the T_1 state. Hence, the measured decay time is longer than that of the prompt fluorescence. In particular, at 300 K, the delayed fluorescence decays with the time constant of τ_{DF}. This mechanism is also effective in other copper(I) complexes with low-lying MLCT excited states and accounts for the relatively short (radiative) emission decay times as compared to a pure triplet state emission.[24−28,31]

Besides the significance for fundamental research, the fact of the strong involvement of the first excited singlet state in the luminescence of copper complexes has also practical implications, in particular, for the use in OLEDs or LEECs. Specifically, if the emission properties were determined only by the lowest triplet state with its long emission decay time of many hundred microseconds, the devices would show only poor performance, for example, because of saturation effects. However, since the singlet state S_1 is thermally populated at ambient temperature, much higher radiative decay rates and higher quantum yields result. For example, for Cu(pop)(pz_2Bph_2) the decay time drops by a factor of almost 40 from 480 μs at T = 40 K to 13 μs at ambient temperature. Consequently, the thermally activated fluorescence strongly dominates the emission. Moreover, if blue light emission is desired, such an activation process is also favorable, since the fluorescence is blue-shifted with respect to the triplet state emission, for example by 10 nm for Cu(pop)(pz_2Bph_2).

Interestingly, a dominant involvement of the singlet excited state in the emission process also allows to harvest all excitons formed in course of an electroluminesce process in the lowest excited singlet state. This can lead to an efficient electroluminescence based on relatively cheap copper compounds. A schematic illustration of the population processes of the excited states and the subsequent light emission is given in Figure 8. After electron−hole recombination, the electroluminescent excitation process leads to one singlet path and three triplet paths that populate the S_1 and T_1 states of the emitter molecule.[18] SOC induced by the metal ion is strong enough to enable fast intersystem crossing. At small $\Delta E(S_1-T_1)$ separations, both up and down ISC processes occur at ambient temperature. Since the radiative rate for a $T_1 \rightarrow S_0$ transition is much smaller than the ISC rates, the excitation, gathered in the triplet state (three triplet paths), is radiatively deactivated dominantly via the S_1 state. The excitation that

dx.doi.org/10.1021/ic200811a |Inorg. Chem. 2011, 50, 8293–8301

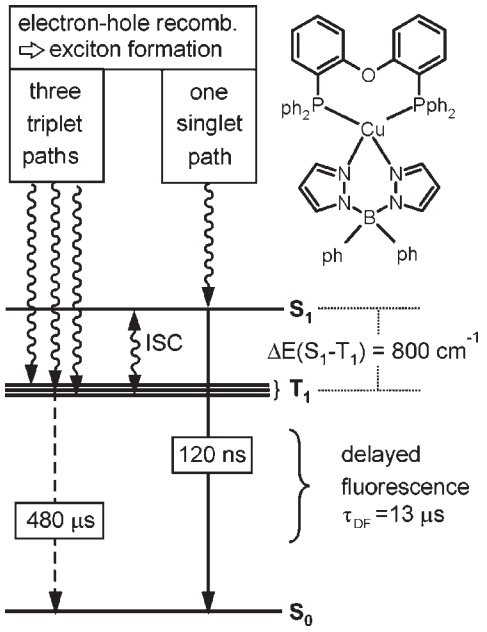

Figure 8. Emission behavior of neat Cu(pop)(pz_2Bph_2) and mechanism of singlet harvesting. At $T \leq 100$ K, the luminescence, with a decay time of 480 μs, stems from the lowest triplet state T_1. At ambient temperature, a thermally activated delayed fluorescence from the lowest singlet state S_1 with a decay time of $\tau_{DF} = 13$ μs is observed, while the decay time of the prompt fluorescence is about 120 ns. In the emitting layer of an electroluminescent device, one singlet and three triplet paths populate the S_1 and T_1 states of the complex. Because of efficient up-intersystem crossing from the T_1 to the S_1 state it is expected that at ambient temperature all excitations can be harvested in the S_1 state and can be used for light generation.

originally populates the singlet state (one singlet path) also takes part in the equilibration process and finally is also deactivated as $S_1 \rightarrow S_0$ emission. Thus, the singlet state harvests all excitons and emits according to its high deactivation rate. Interestingly, a participation of the singlet state in the emission has already been investigated using green to orange light emitting copper complexes.[26,31,51,53,63]

In conclusion, it is remarked that the dominance of the singlet state in the luminescence process can lead to relatively short radiative decay times. A further reduction is, at least in principle, possible by reducing the energy separation $\Delta E(S_1-T_1)$ and/or by increasing the allowedness of the $S_1 \rightarrow S_0$ transition. Such investigations are advantageous for minimizing the efficiency roll-off of an OLED operating under high current densities, as required, for example, for OLED illumination devices.

The Cu(I) complexes studied in this work exhibit high luminescence quantum yields, suitable CIE color coordinates for blue color, and show already relatively short emission decay times. Thus, taking advantage of the singlet harvesting effect, Cu(pop)(pz_2BH_2), Cu(pop)(pz_4B), and Cu(pop)(pz_2Bph_2) seem to be highly interesting for OLED applications.

■ ASSOCIATED CONTENT

Supporting Information. Crystallographic data in CIF format. This material is available free of charge via the Internet at http://pubs.acs.org.

■ AUTHOR INFORMATION

Corresponding Author

*E-mail: hartmut.yersin@chemie.uni-regensburg.de.

Present Addresses

†Department of Chemistry, Clemson University, Clemson, SC 29634, U.S.A.

■ ACKNOWLEDGMENT

The authors thank Dr. Manfred Zabel for X-ray measurements. The German Federal Ministry of Education and Research (BMBF) is acknowledged for the funding of our research.

■ REFERENCES

(1) Yersin, H., Ed.; *Highly Efficient OLEDs with Phosphorescent Materials*; Wiley-VCH: Weinheim, Germany, 2008.

(2) Xiao, L.; Chen, Z.; Qu, B.; Luo, J.; Kong, S.; Gong, Q.; Kido, J. *Adv. Mater.* **2011**, *23*, 926–952.

(3) Borek, C.; Hanson, K.; Djurovich, P. I.; Thompson, M. E.; Aznavour, K.; Bau, R.; Sun, Y.; Forrest, S. R.; Brooks, J.; Michalski, L.; Brown, J. *Angew. Chem., Int. Ed.* **2007**, *46*, 1109–1112.

(4) Lo, S. C.; Harding, R. E.; Shipley, C. P.; Stevenson, S. G.; Burn, P. L.; Samuel, I. D. W. *J. Am. Chem. Soc.* **2009**, *131*, 16681–16688.

(5) Tanaka, D.; Sasabe, H.; Li, Y.-J.; Su, S.-J.; Takeda, T.; Kido, J. *Jpn. J. Appl. Phys.* **2007**, *46*, L10–L12.

(6) Hudson, Z. M.; Sun, C.; Helander, M. G.; Amarne, H.; Lu, Z.-H.; Wang, S. *Adv. Funct. Mater.* **2010**, *20*, 3426–3439.

(7) Kapturkiewicz, A. Electrochemiluminescent Systems as Devices and Sensors. In *Electrochemistry of Functional Supramolecular Systems*; Ceroni, P., Credi, A., Venturi, M., Eds.; John Wiley & Sons: Hoboken, NJ, 2010; p 477.

(8) Wu, C.; Chen, H.-F.; Wong, K.-T.; Thompson, M. E. *J. Am. Chem. Soc.* **2010**, *132*, 3133–3139.

(9) Lo, K. K.-W.; Louie, M.-W.; Zhang, K. Y. *Coord. Chem. Rev.* **2010**, *254*, 2603–2622.

(10) Zhao, Q.; Li, F.; Huang, C. *Chem. Soc. Rev.* **2010**, *39*, 3007–3030.

(11) Botchway, S. W.; Charnley, M.; Haycock, J. W.; Parker, A. W.; Rochester, D. L.; Weinstein, J. A.; Williams, J. A. G. *Proc. Natl. Acad. Sci. U.S.A.* **2008**, *105*, 16071–16076.

(12) Yu, M.; Zhao, Q.; Shi, L.; Li, F.; Zhou, Z.; Yang, H.; Yi, T.; Huang, C. *Chem. Commun.* **2008**, 2115–2117.

(13) Hofbeck, T.; Yersin, H. *Inorg. Chem.* **2010**, *49*, 9290–9299.

(14) Rausch, A. F.; Thompson, M. E.; Yersin, H. *Inorg. Chem.* **2009**, *48*, 1928–1937.

(15) Rausch, A. F.; Thompson, M. E.; Yersin, H. *J. Phys. Chem. A* **2009**, *113*, 5927–5932.

(16) Baldo, M. A.; O'Brien, D. F.; You, Y.; Shoustikov, A.; Sibley, S.; Thompson, M. E.; Forrest, S. R. *Nature* **1998**, *395*, 151–154.

(17) Baldo, M. A.; Lamansky, S.; Burrows, P. E.; Thompson, M. E.; Forrest, S. R. *Appl. Phys. Lett.* **1999**, *75*, 4–6.

(18) Yersin, H. *Top. Curr. Chem.* **2004**, *241*, 1–26.

(19) Kawamura, Y.; Goushi, K.; Brooks, J.; Brown, J. J.; Sasabe, H.; Adachi, C. *Appl. Phys. Lett.* **2005**, *86*, 071104.

(20) Sasabe, H.; Takamatsu, J.; Motoyama, T.; Watanabe, S.; Wagenblast, G.; Langer, N.; Molt, O.; Fuchs, E.; Lennartz, C.; Kido, J. *Adv. Mater.* **2010**, *22*, 50030–5007.

(21) Adachi, C.; Baldo, M. A.; Thompson, M. E.; Forrest, S. R. *J. Appl. Phys.* **2001**, *90*, 5048.

(22) Sajoto, T.; Djurovich, P. I.; Tamayo, A. B.; Oxgaard, J.; Goddard, W. A., III; Thompson, M. E. *J. Am. Chem. Soc.* **2009**, *131*, 9813–9822.

(23) Wagenknecht, P. S.; Ford, P. C. *Coord. Chem. Rev.* **2011**, *255*, 591–616.

(24) Blasse, G.; McMillin, D. R. *Chem. Phys. Lett.* **1980**, *70*, 1–3.

(25) Breddels, P. A.; Berdowski, P. A. M.; Blasse, G.; McMillin, D. R. *J. Chem. Soc., Faraday Trans. 2* **1982**, *78*, 595–601.
(26) Tsuboyama, A.; Kuge, K.; Furugori, M.; Okada, S.; Hoshino, M.; Ueno, K. *Inorg. Chem.* **2007**, *46*, 1992–2001.
(27) Felder, D.; Nierengarten, J.-F.; Barigelletti, F.; Ventura, B.; Amaroli, N. *J. Am. Chem. Soc.* **2001**, *123*, 6291–6299.
(28) Siddique, Z. A.; Yamamoto, Y.; Ohno, T.; Nozaki, K. *Inorg. Chem.* **2003**, *42*, 6366–6378.
(29) Armaroli, N.; Accorsi, G.; Cardinali, F.; Listorti, A. *Top. Curr. Chem.* **2007**, *280*, 69–115.
(30) Giebink, N. C.; Forrest, S. R. *Phys. Rev. B* **2008**, *77*, 235215.
(31) Deaton, J. C.; Switalski, S. C.; Kondakov, D. Y.; Young, R. H.; Pawlik, T. D.; Giesen, D. J.; Harkins, S. B.; Miller, A. J. M.; Mickenberg, S. F.; Peters, J. C. *J. Am. Chem. Soc.* **2010**, *132*, 9499–9508.
(32) Yersin, H.; Monkowius, U. Ger. Patent DE 10 2008 033 563 A1, 2008.
(33) Yersin, H.; Czerwieniec, R.; Monkowius, U. Ger. Patent DE 10 2011 000 406.8, 2011.
(34) Yersin, H. Controlling Photophysical Properties of Metal Complexes: Toward Molecular Photonics. *Book of Abstracts*, COST D35 Workshop, Prague, Czech Republic, May 2010; p. 6.
(35) Altomare, A.; Cascarano, G.; Giacovazzo, C.; Guagliardi, A. *J. Appl. Crystallogr.* **1993**, *26*, 343–350.
(36) Sheldrick, G. M. *SHELXL-97. Program for crystal structure refinement*; University of Göttingen: Göttingen, Germany, 1997.
(37) Sluis, P.; Spek, A. L. *Acta Crystallogr., Sect. A* **1990**, *46*, 194–201.
(38) Aslanidis, P.; Cox, P. J.; Tsipis, A. C. *Dalton Trans.* **2010**, *39*, 10238–10248.
(39) Armaroli, N.; Accorsi, G.; Bergamini, G.; Ceroni, P.; Holler, M.; Moudam, O.; Duhayon, C.; Delavaux-Nicot, B.; Nierengarten, J.-F. *Inorg. Chim. Acta* **2006**, *360*, 1032–1042.
(40) Monkowius, U.; Ritter, S.; König, B.; Zabel, M.; Yersin, H. *Eur. J. Inorg. Chem.* **2007**, 4597–4606.
(41) Yersin, H.; Czerwieniec, R.; Monkowius, Uwe; Yu, J. Patents WO002010031485A1, DE102008048336A1, 2008.
(42) Xie, Y.-M.; Wu, J.-H. *Inorg. Chem. Commun.* **2007**, *10*, 1561–1564.
(43) Vorontsov, I. I.; Graber, T.; Kovalevsky, A. Y.; Novozhilova, I. V.; Gembicky, M.; Chen, Y.-S.; Coppens, P. *J. Am. Chem. Soc.* **2009**, *131*, 6566–6573.
(44) Shaw, G. B.; Grant, C. D.; Shorota, H.; Castner, E. W., Jr.; Meyer, G. J.; Chen, L. X. *J. Am. Chem. Soc.* **2007**, *129*, 2147–2160.
(45) Sakaki, S.; Mizutani, H.; Kase, Y. *Inorg. Chem.* **1992**, *31*, 4575–4581.
(46) Cunningham, C. T.; Moore, J. J.; Cunningham, K. L. H.; Fanwick, P. E.; McMillin, D. R. *Inorg. Chem.* **2000**, *39*, 3638–3644.
(47) Turro, N. J. *Modern Molecular Photochemistry*; Benjamin Inc.: Menlo Park, CA, 1978.
(48) Siebrand, W. *J. Chem. Phys.* **1967**, *46*, 440–447.
(49) Stufkens, D. J.; Vlček, A., Jr. *Coord. Chem. Rev.* **1998**, *177*, 127–179.
(50) Caspar, V.; Kober, E. M.; Sullivan, B. P.; Meyer, T. J. *J. Am. Chem. Soc.* **1982**, *104*, 630–632.
(51) Zhang, Q.; Zhou, Q.; Cheng, Y.; Wang, L.; Ma, D.; Jing, X.; Wang., F. *Adv. Mater.* **2004**, *16*, 432–436.
(52) Smith, C. S.; Branham, C. W.; Marquardt, B. J.; Mann, K. R. *J. Am. Chem. Soc.* **2010**, *132*, 14079–14085.
(53) Zhang, Q.; Ding, J.; Cheng, Y.; Wang, L.; Xie, Z.; Jing, X.; Wang, F. *Adv. Funct. Mater.* **2007**, *17*, 2983–2990.
(54) Smith, T.; Guild, J. *Trans. Opt. Soc.* **1931/32**, *33*, 73–130.
(55) For Cu(pop)(pz_2BH_2), the experimental decay profile at 1.6 K could be fitted biexponentially with decay components of 300 μs and 2.8 ms. However, in view of the results obtained for the other two compounds, **2** and **3**, a third decay component of several hundred microseconds should be present. Its value can be estimated. For $\Delta E(\mathrm{ZFS}) \ll k_B T$ with k_B being the Boltzmann constant, an average decay time (τ_{therm}) of the three equilibrated T_1 substates can be expressed by $\tau_{therm} = 3(1/\tau_I + 1/\tau_{II} + 1/\tau_{III})^{-1}$, wherein τ_I, τ_{II}, and τ_{III} represent the individual decay components of the triplet substates I, II, and III, respectively.[57,58] If we identify the decay time measured between 30 and 100 K (plateau with ≈ 610 μs; Figure 7) as τ_{therm} and τ_I and τ_{III} as the decay components of 2.8 ms and 300 μs, respectively, a value of $\tau_{II} \approx 1$ ms is obtained.
(56) (a) Yersin, H.; Finkenzeller, W. J. In *Highly Efficient OLEDs with Phosphorescent Materials*; Yersin, H., Ed.; Wiley-VCH: Weinheim, Germany, 2008; pp 1−97. (b) Yersin, H.; Rausch, A. F.; Czerwieniec, R.; Hofbeck, T.; Fischer, T. *Coord. Chem. Rev.* **2011**, doi:10.1016/j.ccr.2011.01.042.
(57) Yersin, H.; Strasser, J. *Coord. Chem. Rev.* **2000**, *208*, 331–364.
(58) Yersin, H.; Donges, D. *Top. Curr. Chem.* **2001**, *214*, 81–186.
(59) Rausch, A. F.; Homeier, H. H. H.; Yersin, H. *Top. Organomet. Chem.* **2010**, *29*, 193–235.
(60) Murov, S. L.; Carmichael, J.; Hug, G. L. *Handbook of Photochemistry*, 2nd ed.; Marcel Dekker: New York, 1993; p 340.
(61) Czerwieniec, R.; Finkenzeller, W. J.; Hofbeck, T.; Starukhin, A.; Wedel, A.; Yersin, H. *Chem. Phys. Lett.* **2009**, *468*, 205–210.
(62) The energies of the S_1 and T_1 states of the pop ligand, as determined from flanks of the luminescence spectra measured in dilute ethanol/methanol solutions at ambient temperature and at 77 K, respectively, are $E(S_1) = 34300$ cm^{-1} and $E(T_1) = 27600$ cm^{-1}. For the oxidized pop ligand, bis(2-(diphenylphosphino)phenyl ether dioxide, $E(S_1)$ and $E(T_1)$ are 34000 cm^{-1} and 28100 cm^{-1}, respectively.
(63) Che, G.; Su, Z.; Li, W.; Chu, B.; Li, M.; Hu, Z.; Zhang, Z. *Appl. Phys. Lett.* **2006**, *89*, 103511.